https://doi.org/10.1016/j.nanoen.2021.105873

4D-printed Self-Recovered Triboelectric Nanogenerator for Energy Harvesting and Self-Powered Sensor

Long-Biao Huang[a,1,*], Jian-Cheng Han[a,1], Shaojun Chen[b], Zhenhua Sun[a], Xingyi Dai[a], Penghui Ge[b], Cheng-Han Zhao[a], Qiu-Qun Zheng[a], Fu-Chun Sun[c,*], Jianhua Hao[d,*]

[a] Key Laboratory of Optoelectronic Devices and Systems of Ministry of Education and Guangdong Province, College of Physics and Optoelectronic Engineering, Shenzhen University, Shenzhen, 518060, P. R. China
* Corresponding Author E-mail: huanglb@szu.edu.cn

[b] College of Materials Science, Shenzhen University, Shenzhen, 518060, P. R. China

[c] State Key Lab of Intelligent Technology and Systems, Department of Computer Science and Technology, Tsinghua University, 100084, Beijing, P. R. China
* Corresponding Author E-mail: fcsun@tsinghua.edu.cn

[d] Department of Applied Physics, The Hong Kong Polytechnic University, Hong Kong, P. R. China
* Corresponding Author E-mail: jh.hao@polyu.edu.hk

Abstract

Based on the triboelectrification and electrostatic induction, triboelectric nanogenerators (TENGs) have already expanded many applications ranging from ambient mechanical energy harvesting to self-powered sensors. Diverse advanced techniques have been utilized to fabricate various devices to fulfill those applications. To further develop the wide utilization of TENGs, we introduce 4D printing technology to fabricate the transparent self-recovered TENGs, which not only provide excellent self-recoverability of device performance and improve the robustness of device structure, but also open a path to fabricate complicated structure through computer design with no need of any molds. The printed devices have the capabilities of harvesting mechanical energy with maximum output power density of 56 mW/m^2 as well as detecting the bending angles of human joints as self-powered sensor. The self-recoverability is originated from shape memory polymer (SMP) under thermal treatment. Therefore, the self-recovered TENGs based on 4D printing technology may offer great potential in energy harvesting and self-powered sensors for human-robot cooperation in sensing and control of robot in need of sophisticated and precise structures.

Keywords: Triboelectric nanogenerators, 4D printing technology, Shape memory polymer, Self-powered sensor

Highlights

- A novel 4D printed TENG was firstly achieved by combination 3D printing technique and shape memory materials.
- The 4D-printed microstructure and whole TENG device has the excellent self-recover property in short time.
- Different working modes of TENGs could be easily fabricated through computer design.
- The 4D- printed TENG could be utilized to harvest mechanical energy and detect bending angles of human joints as a self-powered sensor.

1. **Introduction**

Triboelectric nanogenerators (TENGs) have attracted increasing interests for both scavenging mechanical energy from environment and self-powered systems [1-4].Due to the coupling effect of triboelectrification and electrostatic induction in different tribomaterials, TENGs can easily convert mechanical motion into electricity or electric signals [5-7]. Comparing with other technologies, TENGs have already shown many advantages, such as easy-fabrication, low-cost, diverse working modes and high power conversion efficiency, etc [8-10].

In order to harvest energy with high efficiency and generate electric signal from various detected system, different complex structure of TENG device had been designed and fabricated with diverse techniques [11-15]. At the same time, to generate electricity or electric signal, the polymer materials as key constituents in TENG device must withstand impact and friction with electrodes under external mechanical motions [16-20]. Unfortunately, those impacts and friction generate severe deformation of polymer materials which could lead to decrement of device's output performance. Therefore, one of obvious obstacles limiting further applications of TENGs is how to construct complicated structure in TENG device and maintain high performance of the device [21-23].

In order to facilitate the realization of sophisticated and precise TENG devices, printing technology has been emerged and shown an improvement in the manufacturing efficiency. The advanced method has been employed to fabricate complicated structure and therefore extended to various applications [24-29]. Among those techniques, 3D

printing method through computer design can directly fabricate complicated structure with diverse materials without any molds. The utilization of 3D printing technology for TENGs had been chosen and achieved intriguing results by several groups [30-32]. Wang et al. demonstrated 3D printing technology to provide ultraflexible 3D TENG which can generate 10.98 W/m^3 and 0.65 mC/m^3 under low frequency of 1.3Hz [30]. Baik et al. utilized 3D printer to fabricate a fully-packaged, cylinder-shaped TENG device which may work under harsh environments to generate output power of 45 mW [31]. Cellulose aerogel had been employed in 3D-printed TENG as tribomaterials and the formed 3D micro/nano patterned structure can significantly improve the output performance of TENG due the increased contact area and surface roughness [32]. However, due to the impact and friction under external mechanical motion, the 3D printed device might suffer from the degradation or loss of output performance and even fully damaging of device [24, 26, 27, 30]. Therefore, the robustness and reliability of 3D printed TENG must be considered for the future applications. However, there has been limited report on this topic so far.

To maintain or improve the robustness and reliability of TENGs, a variety of feasible strategies had been utilized including noncontact mode, liquid-solid contact, self-recovery and rolling structural TENG [22, 33, 34]. In those strategies, self-recovery TENG based on self-healing and shape-memory materials had shown the capability of molecular structure repaired to improve long-term serving and reliability of devices [35-37]. Xu et al. reported a fully self-healing TENG by utilizing a healable polymer into device which achieved above 95% of initial value after recovery [38]. Lee et al.

demonstrated an TENG based shape-memory polymer which had capability to recovery the micropatterns by heating at 55 ºC [33]. In those materials, the utilization of shape-memory polymer may provide a feasible way to solve above obstacles, and show great flexibility in engineering processes of materials and device design.

Comparing with traditional 3D printing technique, 4D printing technology takes an advantage of smart materials to design and fabricate diverse intelligent device with complicated structure.[39-44] The shape, property and functionality of 4D-printed object have the capability to evolve with time under an external stimuli [45-48]. Gladman et al. had utilized hydrogel composite ink for 4D printing. Through optimization of printing parameters, a double-layer structure with programmable anisotropy was achieved to be transformed into the target shape while immersed in water [44]. Kuang et al. combined shape-memory and self-healing properties into 4D printing technique. The 4D-printed spiral could be cut and stretched into a broken strip as a temporary shape. Once heated above 70 ºC, the broken area can be self-healed and recovered to its original structure [49]. Therefore, 4D printing technique combining the advantages of 3D printing technology and shape-memory materials, may pave the way of developing durable TENGs enjoying complicated and precise structures.

Herein, a novel 4D printed triboelectric nanogenerators (4DP-TENG) based on shape-memory polymer with sprayed electrodes of silver nanowires are designed and fabricated by fused deposition modeling (FDM) printer and spray technique in this work. The research results present that the printed microstructure and whole TENG device can be readily recovered simply by thermal treatment at 60 ºC in the oven. Our

4DP-TENG with the contact-separated and freestanding modes are effectively utilized to harvest mechanical energy. The optimized freestanding mode-based 4DP-TENG can detect human motion of finger, wrist and elbow joints at different bending angles. The results in the present study prove 4D printed technology to be a powerful technique in the fabrication of TENGs for harvesting mechanical energy and self-powered human motion sensors, showing great potential for human-robot cooperation in sensing and control of robot in need of sophisticated and precise structures.

2. Experimental Section

2.1 Raw Materials

Silver nitrate ($AgNO_3$, 99.8%), ethylene glycol (EG), polyvinylpirrolidone (PVP, 360 k), copper chloride ($CuCl_2{:}2H_2O$), poly(ethylene-glycol-adipate) diols, diphenylmethane diisocyanate, dibutyl tin dilaurate, absolute ethanol and other chemicals were purchased from Aladin and used without further purification.

2.2 Preparation of Silver Nanowires (AgNWs)

Firstly, 0.3 mg of $CuCl_2{:}2H_2O$ were dispersed in 50 ml of EG. Subsequently, 250 mg of $AgNO_3$ in 15 ml of EG were mixed in previous solution. Subsequently, 15 ml of EG with 190 mg of PVP were dropped by peristaltic pumping with a rate of 2 ml/min. When the solution was fully changed from transparent to pearly, the AgNWs were synthesized in solution. The centrifuges were utilized to separate the AgNWs from EG and other

chemicals at 1500 rpm. Then, the collective AgNWs were redistributed in absolute ethanol (25 ml) and installed in the spray machine (Dragon Nation, LB-NMH186A).

2.3 Preparation of Shape-Memory Polymer (SMP) Filament

The SMP filament is prepared as follows. 90 g Poly(ethylene-glycol-adipate) diols were mixed with diphenylmethane diisocyanate and diethylene glycol with 10 wt%. After adding 0.1g dibutyl tin dilaurate as catalyst, the mixture was heated at 60 ^{o}C under stirring. After curing at 120 ^{o}C for about 12 h, polyurethane prepolymer (PU) with high molecular weight was dried in a vacuum-drying oven (Shanghai Pein Experimental Instrument Co., Ltd., China) at 90 ^{o}C for 10 h. Then, polyurethane/polylactic acid composite with 5:5 was synthesized by mixing extrusion at 220 ^{o}C to obtain raw materials for extrusion. The FHD filaments were fabricated by a double screw extruder (XH-433-40, Dongguan Xihua Machine Co., Ltd., China) with optimization parameter to ensure the diameter (1.75 mm), density and ratio. FDM 3D printer (Ultimaker S3) was utilized to print the specimens with printing speed 35 mm/s, printing temperature 210 ^{o}C, filling rate 100 % and substrate temperature 45^{o}C on the paper tape which could provide good adhesion between polymer and substrate.

2.4 Fabrication of TENGs

Contact-separation and freestanding mode-based TENGs were designed and fabricated by fused deposition modeling 3D printer.

2.5 Characterization

The scanning electrons microscopy (SEM) images were acquired by a Field Emission Scanning Electron Microscope (JSM-6701F, JEOL) to investigate the surface morphology of devices and AgNWs. The output performance of TENGs including open-circuit voltage (V_{oc}), short-circuit current (I_{sc}) and transferred charge (Q_c) were measured and analyzed by LeCroy Wave Runner Oscilloscope (44MXI) with probe resistance value of 10 MΩ, SR570 low noise current amplifier (Stanford Research System) and 6514 system electrometer (Keithley), following previous literatures [50, 51].

3. Results and Discussion

The 4FP-TENGs were designed and fabricated by Fused Deposition Modeling (FDM) printer with SMP filaments. The devices and electrodes were fabricated as depicted in **Figure 1**. Under the motor driving, the SMP filament was heated at 210 ºC in the printer head and extruded through a small opening as shown in **Figure 1a**. The print bed was kept at 45 ºC to prevent the device from cooling too fast. The printing speed at X and Y direction was fixed at 35 mm/s, while printing speed at Z direction was 0.1 mm/min. The surface morphology of fused deposited SMP film is presented in **Figure 1C**, in which the microwires of SMP were printed. The final printed triboelectric materials are presented in the inset of **Figure 1a** which show significant transparent character of SMP. The electrodes of TENGs are fabricated by spray machine as shown

in **Figure 1b**. Due to high temperature of printing bed and hot deposited SMP filament, ethanol could be evaporated in short time and the AgNWs could form conductive electrode of TENGs as shown in **Figure 1d**. Through the design of device structure, two working modes of TENGs including contact-separation and freestanding mode can be fabricated. As the SMP can recover to its original shape, the printed triboelectric materials may enjoy self-recovery properties and form 4DP-TENGs.

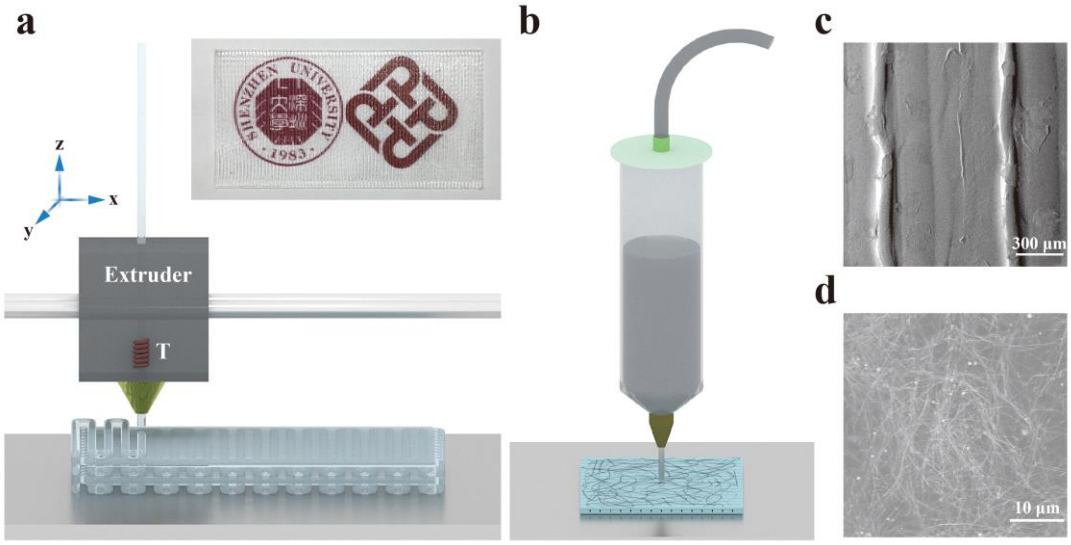

Figure 1. Schematically illustration of 4DP-TENG: a) fabrication of supporting and triboelectric materials; b) fabrication of AgNWs electrode, c) SEM image of polymer surface morphology; d) SEM image of AgNWs electrode.

Followed by the processing of 4DP-TENGs, the self-recovery properties of device were investigated as shown in **Figure 2**. The operation of TENGs relies on the coupling effect of triboelectrification and electrostatic induction which results from sufficiently contact of two different materials. The external impact could damage the microstructure

of the constituent materials and main construction of device and lead to the degradation of output performance. Therefore, the incorporation of self-recovery properties into device will benefit for long-term operation of TENGs. As shown in **Figure 2a**, the SEM and optical images present surface morphology with high surface area at original stage which is similar with the literature [27]. After hundreds of impacts, the SEM and optical images show serious deformation of microstructure and main structure. Microwires of SMP had fully collapsed, and the main structure of SMP in the inset of **Figure 2b** folded after releasing external force. To recovery the microstructure and main structure of the TENG, the whole device was storage in oven with 60 ^{o}C. After 30 s, the microstructure and main structure are fully recovered, which are similar with their original states as shown in **Figure 2c**.

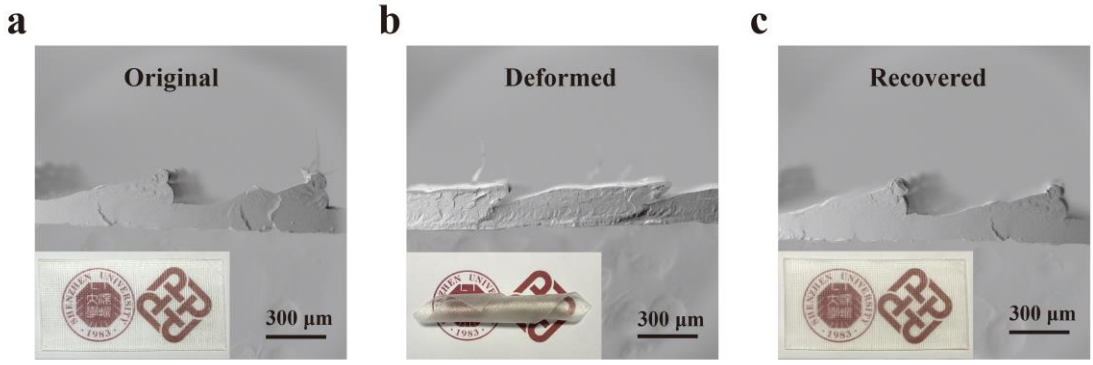

Figure 2. Cross-section SEM images of 4D printed SMP film: a) Original state, b) Deformed state, c) Recovered state.

In this study, two working modes including contact-separation and freestanding are adopted for diverse applications. Firstly, the working principle and output performance

of contact-separation 4D-printed TENG are studied as shown in **Figure 3**. The tribomaterials and device supporting materials are fully printed using SMP, and the conducting electrode is formed by a sprayer in **Figure 3a**. Under external force, the AgNWs electrode could contact with printed SMP tribomaterials in **Figure 3b-ii**. Due to the differences in triboelectric polarities between SMP and AgNWs, electrons could be attracted on the surface of SMP. After the separation as shown in **Figure 3b-iii**, the positive charge on the AgNWs electrodes and negative charges on the surface of SMP could be formed and created electrical potentials between two AgNWs electrodes which lead to the instantaneous electricity. By repeating the contact and separation processes, the alternating current is created to fulfill the conversion of external mechanical energy.

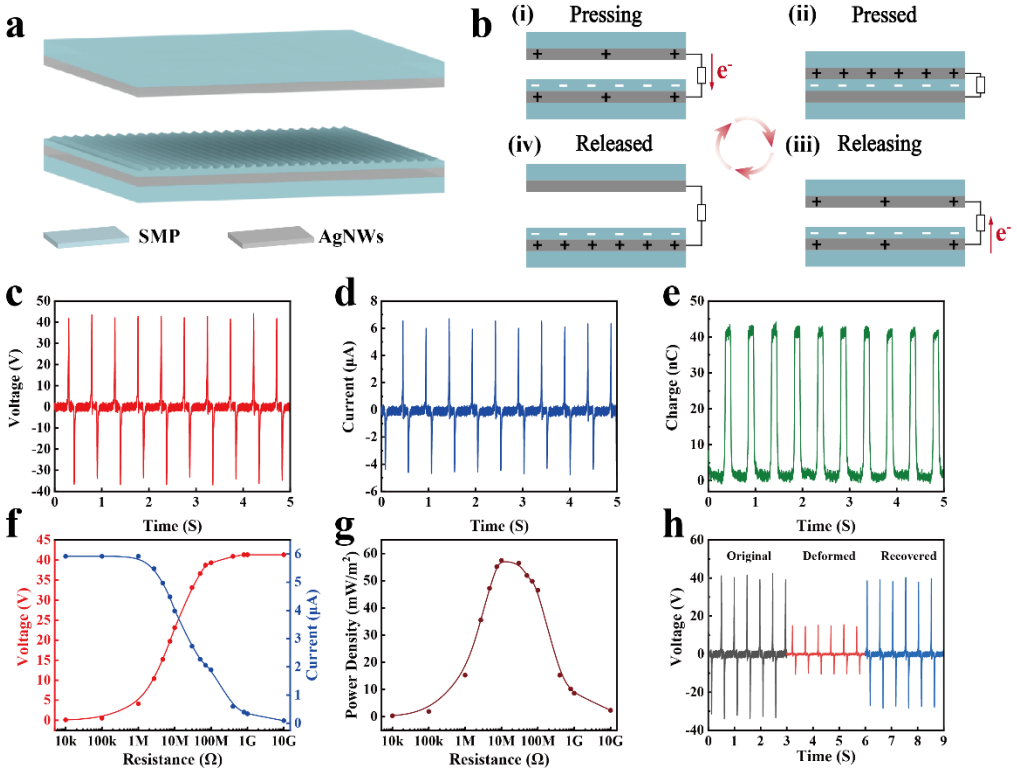

Figure 3. (a) and (b) schematically illustration of device structure and working principles of contact-separation 4DP-TENG, respectively. (c) Open-circuit voltage, (d)

short-circuit current, and (e) transferred charge of contact-separation 4DP-TENG with a frequency of 2 Hz. (f) Output voltage and current versus resistance of contact-separation 4DP-TENG. (g) Variation of power density with external resistance. h) Performance comparison of original, deformed and recovered device

To evaluate the energy harvesting capability of contact-separation 4DP-TENG, the device with 4 cm×4 cm was printed to harvest mechanical energy under 128 N force. The output performance of device is presented in **Figure 3**. The V_{oc}, I_{sc} and Q_c of contact-separation mode arrive at 39 V, 5.9 μA and 43 nC, respectively. In Figure 3e, the voltage across the load resistance increases with increment of resistance, while current flowing through the load resistance presents a reverse trend The maximum output power density of the prepared device can achieve at 56 mW/m^2 with external resistance of ~ 10 MΩ as shown in **Figure 3g**. After several hundreds of impacts, the V_{oc} decreased to 18 V and about 50% of original device which could be attributed to the change of the surface morphology of 4DP-TENG. The surface morphology was deformed and had less surface area comparing with original state as shown in **Figure 2**. After thermal treatment at 60 ^{o}C for about 1 min, the surface morphology could be recoved, providing enough surface area for TENG. As shown in **Figure 3h**, V_{oc} of self-recovered device can achieve at 38 V which is very close to 40 V measured from original device.

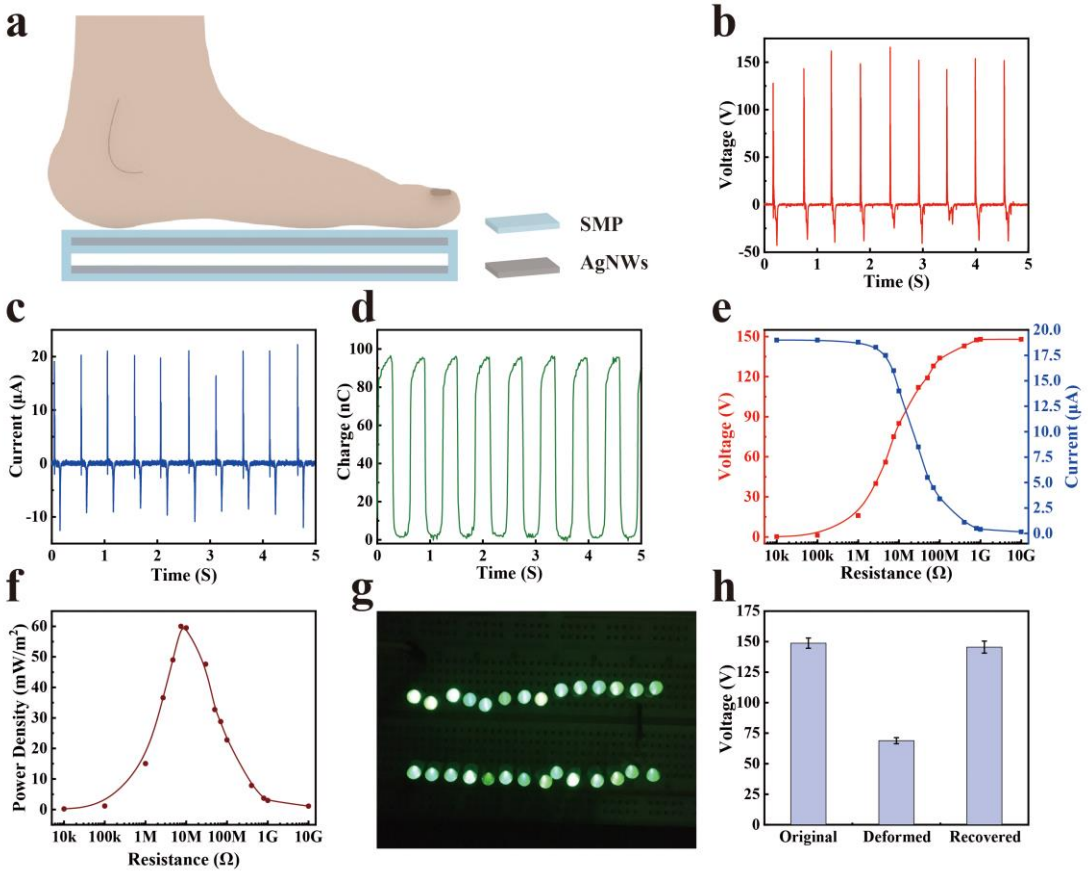

Figure 4. (a) Schematically illustration of 4D printed contact-separation mode TENG for walking energy harvesting. (b) Open-circuit voltage, (c) Short-circuit current, (e) Transferred charge, (e) Dependence of output performance and (f) peak power of contact-separation mode triboelectric nanogenerator on the resistance of external load, respectively. (g) Images of 28 green LEDs powered by contact-separation 4DP-TENG without external circuit loads, (h) Open-circuit voltage of contact-separation 4DP-TENG at original, deformed and recovered state.

For practical harvesting of human walking energy[7, 52, 53], the insole with 7.5 size in US size was designed and fabricated into contact-separation mode TENG as shown

in **Figure 4a**. Under 60 Kg pressuring of human, V_{oc}, I_{sc} and Q_c of contact-separation mode TENG are measured to be 140 V, 19 uA and 95 nC in 2 Hz, respectively. The value of V_{oc} increases with increment of resistance, while I_{sc} decreases. The maximum output power density of prepared device can achieve at 56 mW/m^2 with external resistance of ~ 7 MΩ as shown in **Figure 4f**. The whole insole could easily light 28 LEDs in **Figure 4g**. After several hundreds of impact, the V_{oc} decreased to 68 V and about 50 % of original device which could be attributed to the change of the surface morphology of 4DP-TENG. The surface morphology was deformed and had less surface area comparing with original state as shown in **Figure 2**. After thermal treatment at 60 ^oC for about 2 min, we found the recovery of surface morphology possessing enough surface area for TENG. As shown in **Figure 4h**, V_{oc} of self-recovered device can achieve at 135 V which is almost same with original device of 138 V.

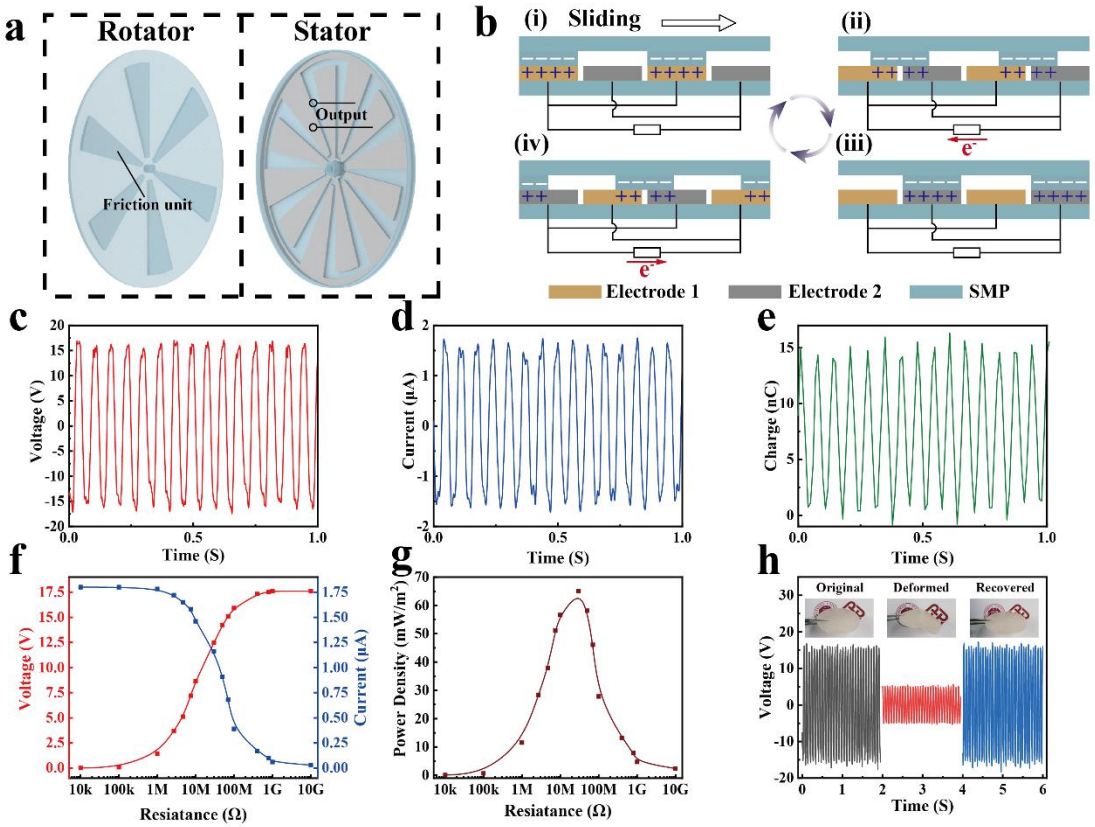

Figure 5. (a) and (b) Schematically illustration of device structure and working principles of 4D-printed freestanding mode TENG, respectively. (c) Open-circuit voltage, (d) short-circuit current, and (e) transferred charge of 4D-printed freestanding mode TENG at 150 rpm. (f) Output voltage and current versus resistance of 4D-printed freestanding mode TENG. (g) Variation of power density with external resistance. (h) Performance comparison of original, deformed and recovered device

It is known that both contact-separation mode TENG and freestanding mode TENG have been extensively used for harvesting of mechanical energy and detection of different motions. To present the usefulness of 4DP-TENG, the freestanding mode device with grating disc structure is designed as shown in **Figure 5a**. The whole device includes two parts: stator with electrode layer and rotator with printed structural support

which provide the alignment of device. Grating structures are printed on the surface of stator and rotator. AgNWs layer was printed on the grating structure surface of stator and formed the electrode layer. 6 blades grating configuration as a demonstration is selected to harvest energy and detect human motion. The working principle of freestanding mode TENG with grating configuration could be attributed to the coupling effect of contact electrification and in-plane-sliding induced charge transfer in **Figure 5b**. Fully overlapping position is the first stage with fully contact between grating of SMP and the fingers of electrode layer in **Figure 5b-i**. Due to the triboelectrically difference between SMP polymer and AgNWs electrode, the contact electrification could lead to the formation of negative charges on the polymer surface and positive charge on the electrodes. When the SMP polymer slides rightward, an electrical potential difference is generated and drives electronic flow between nearby electrodes which lead to a transient current in **Figure 5b-ii**. An electrostatic equilibrium could be achieved after fully overlapping position between SMP polymer and AgNWs electrodes in **Figure 5b-iii**. When the rotator continues to slide, the electrons could flow back and lead to generation of a reverse current in external circuit as shown in **Figure 5b-iv**.The grating disk type of TENG at 150 rpm was 4D-printed and utilized to harvest mechanical energy as shown in **Figure 5c-5e**. The V_{oc}, I_{sc} and Q_c of freestanding mode could arrive at about 16 V, 1.6 μA and 14 nC, respectively. In **Figure 5f**, the voltage across the load resistance increases with increment of resistance, while current flowing through the load resistance presents a reverse trend. The maximum output power density of prepared device can achieve at about 65 mW/m^2 with external resistance of

~ 30 MΩ as shown in **Figure 5g**. After hundreds of period rotations, V_{oc} decreases to about 5 V which is about 35% of original device, due to the deformation of the device structure and the surface morphology. After thermal treatment at 60 ^{o}C for about 1 min, the whole printed device structure could recovery and provide enough surface area for TENG. As shown in **Figure 5h**, the whole structure can recover to the original state under thermal treatment while the V_{oc} of self-recovered device can achieve at about 16 V, which is almost same with original device. It is worth noting that the printed FS mode TENG in **Figure 5h** has lost transparency comparing with printed SMP film in **Figure 1a**. Firstly, the SMP film presented in **Figure 1a** is a thin film with a thickness about 0.2mm. However, in order to ensure the robustness of the self-powered sensor, it is necessary to increase the thickness of the substrate so that the self-powered sensor loses its transparency. Secondly, SMP film in **Figure 2a** is a pure film without silver nanowires. In contrast, the SMP structure for self-powered sensor have the silver nanowire electrodes as conducting layer which also affect the transparency of the device.

In recent years, human-robot cooperation has attracted lots of attentions due to wild applications in manufacturing industry and extreme environments. Self-powered sensor based on TENG had already shown great potential in sensing and control of robot [54-56]. Herein, the self-powered angle-sensor based on 4D-printed freestanding TENGs was fabricated as illustrated in **Figure 6**. By design of the 4D-printed freestanding TENG, device with different sizes are printed and assembled as self-powered human motion angle-sensor. Under driven of human joints in **Figure 6b**, the device could

perform the sliding motion between tribomaterials and electrodes, by recognizing the phase of output signal, we can get the angle information of the joint motion. The working principle of 4D-printed self-powered human motion angle-sensor is schematically illustrated in **Figure 6c** and **Figure 6d**. In the **Figure 6c-i** and **6c-iii**, there are equal amount positive charge on two electrodes, leading to zero electric potential difference between two electrodes. When the friction unit fully overlap with electrode 2 in **Figure 6c-ii**, the positive charge completely transfer to electrode 2 to achieve the electrostatic balance that the electric potential difference between two electrodes reaches the maximum. Due to the coupling effect of contact electrification and in-plane-sliding induced charge transfer, the flexion/extension of joints could be translated into positive or negative pulse signal by angle-sensor as shown in **Figure 6d**. The different phase of output signal presents the variation in the bending angle due to the 6-blades design, specifically a phase of π for 30^{o}, 2π for 60^{o} and 3π for 90^{o} are as shown in **Figure 6d-i** to **6d-iv**.

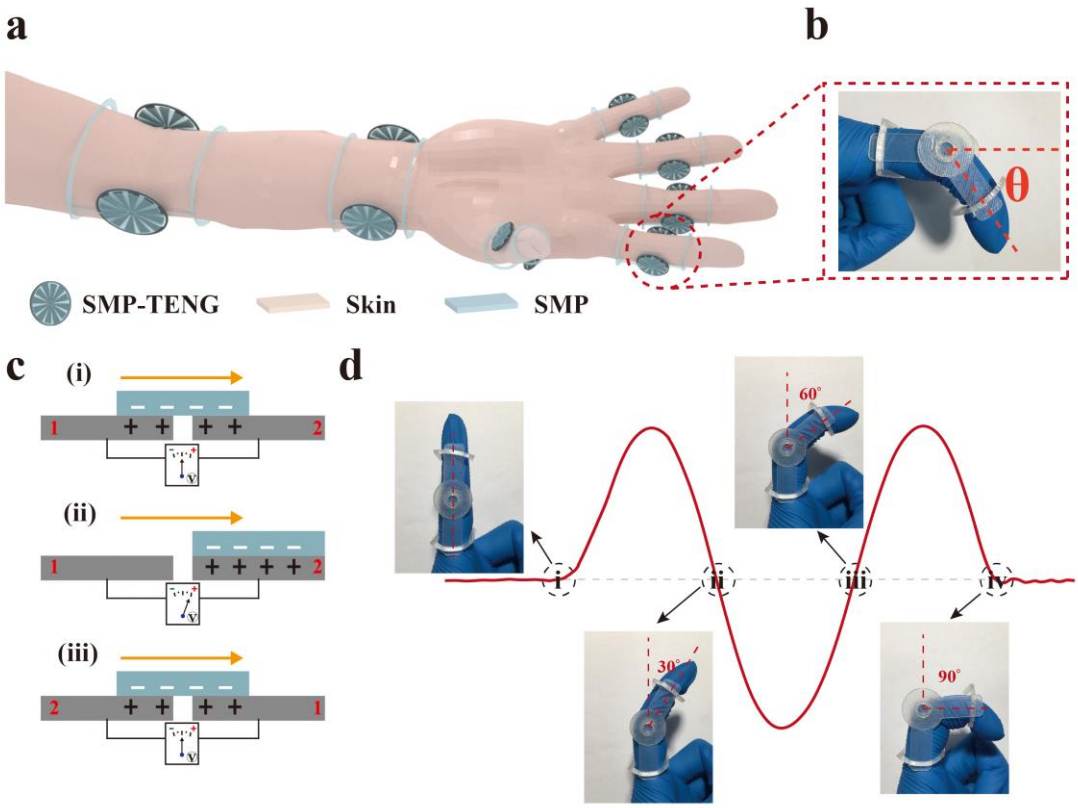

Figure 6. (a) Schematically illustration of self-powered human motion angle-sensor based on 4DP-TENG, (b) finger motion, (c) working principles of sensor, (d) relationship of the Voc and finger motion.

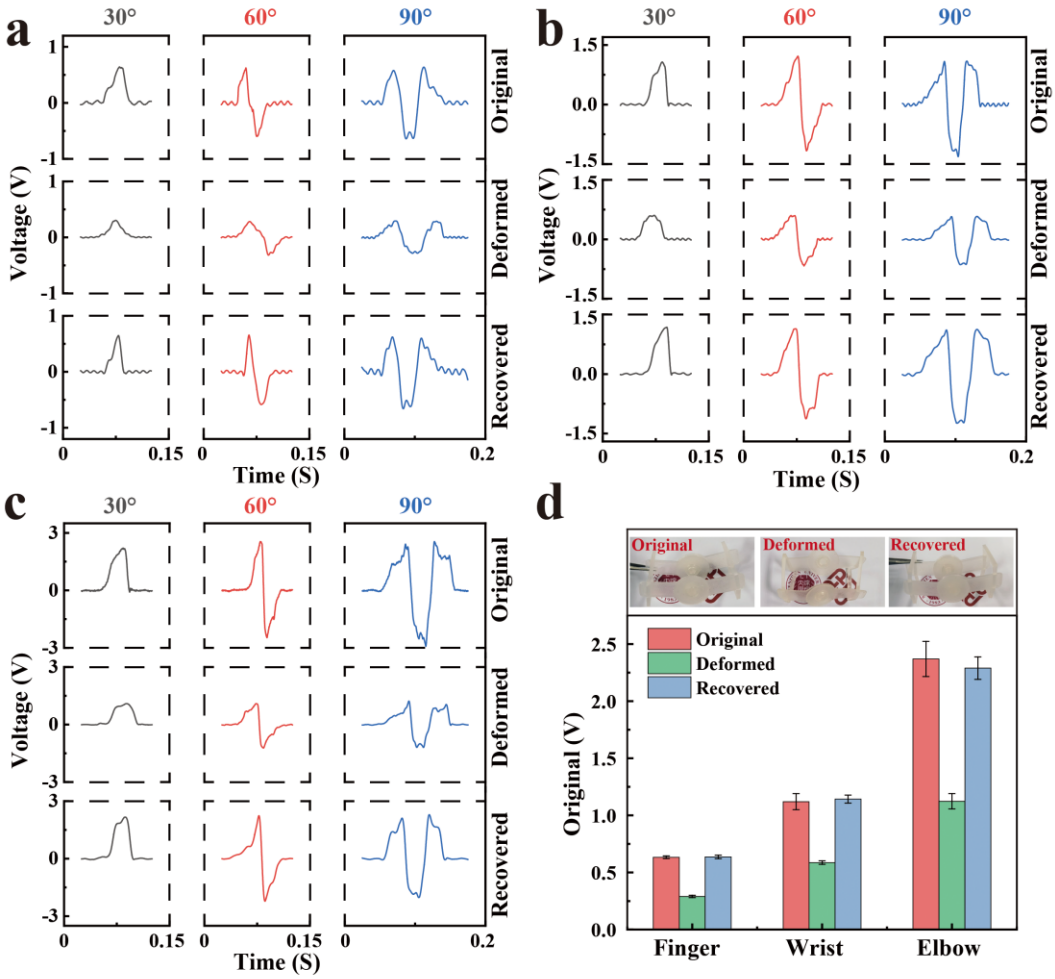

Figure 7. Applications of 4DP-TENG as self-powered human motion angle-sensor to detect (a) finger joints, (b) wrist joints, and (c) elbow joints. (d) Comparison of output performance of original, deformed and recovered angle-sensor.

The 6 blades grating configuration with different device diameters including 15 mm, 20 mm and 30 mm are chosen to detect the bending angle of different joints as shown in **Figure 7**. As mentioned above, all sensors with the 6 blades grating configuration could be utilized to identify the 30°, 60°, 90°, responding to relative phase π、2π and 3π. As shown in **Figure 7a**, the bending angle with 30°, 60°, and 90° of finger joints

could be detected by original angle-sensor with peak value of V_{oc} about 0.6 V. At the same time, the bending angle with 30°, 60°, and 90° of wrist joint and elbow in **Figure 7b** and **7c** could be also detected by original sensors with peak values of V_{oc} about 1.1 V and 2.3 V, respectively. After hundreds of operations, the surface morphology of self-powered sensor could be changed with less surface area which lead to decrement of peak value as shown in **Figure 7a-7d**. Although the deformed angle sensor of wrist joint and elbow could also detect the bending angle with 30°, 60°, and 90°, the peak value of V_{oc} decreased to about 0.3 V, 0.5 V and 1.1 V, respectively. After thermal treatment of 1 min at 60 °C, the surface morphology of deformed angle sensor and the main structure can restore to its original state which leads to performance recovery of self-powered angle sensor in **Figure 7d**. Recently, Wang et al. introduced the self-powered angle sensor at nanoradian-resolution for robotic arms by optimization the grate configuration [54]. By decrement of grating width, the resolution angle of self-powered angle sensor could be further enhanced. Herein, the novel self-recovered TENGs based on 4D printing technology could provide great potential in energy harvesting and self-powered angle sensors for human-robot cooperation in sensing and control of robot with durable, sophisticated and precise structures.

4 Conclusion

To further develop the utilization of TENGs, we demonstrate the self-recovered TENGs fabricated by 4D printing technology, which not only provide excellent self-

recoverability of device performance and robustness of device structure, but also can directly fabricate complicated structure with diverse materials through computer design without any molds. The printed device can harvest mechanical energy with maximum output power density of 56 mW/m^2. Moreover, it is capable of detecting the bending angles of human joints as self-powered sensor. The self-recoverability originated from shape-memory polymer provide excellent self-recoverability of device performance and robustness of device structure after thermal treatment. The novel self-recovered TENGs based on 4D printing technology could provide great potential in energy harvesting and self-powered angle sensors for human-robot cooperation in sensing and control of robot.

Acknowledgements

The research was financially supported by the National Natural Science Foundation of China through grants (51973119), the Natural Science Foundation of Guang Dong Province (2018A0303130060 and 2019A1515011566), the Science and Technology Innovation Commission of Shenzhen City (JCYJ20170818101245583).

References

[1] F.-R. Fan, Z.-Q. Tian, Z.L. Wang, Flexible triboelectric generator! *Nano Energy* 1 (2012) 328-334.

[2] W. Xu, H. Zheng, Y. Liu, X. Zhou, C. Zhang, Y. Song, X. Deng, M. Leung, Z. Yang, R.X. Xu, Z.L. Wang, X.C. Zeng, Z. Wang, A droplet-based electricity generator with high instantaneous power density. *Nature* 578 (2020) 392-396.

[3] H. Zou, Y. Zhang, L. Guo, P. Wang, X. He, G. Dai, H. Zheng, C. Chen, A.C. Wang, C. Xu, Z.L. Wang, Quantifying the triboelectric series. *Nat. Commun.* 10 (2019) 1427.

[4] G. Liu, S. Xu, Y. Liu, Y. Gao, T. Tong, Y. Qi, C. Zhang, Flexible Drug Release Device Powered by Triboelectric Nanogenerator. *Adv. Funct. Mater.* 30 (2020) 1909886.

[5] L. Cheng, Q. Xu, Y. Zheng, X. Jia, Y. Qin, A self-improving triboelectric nanogenerator with improved charge density and increased charge accumulation speed. *Nat. Commun.* 9 (2018) 3773.

[6] Y. Zi, S. Niu, J. Wang, Z. Wen, W. Tang, Z.L. Wang, Standards and figure-of-merits for quantifying the performance of triboelectric nanogenerators. *Nat. Commun.* 6 (2015) 8376.

[7] Y. Zou, V. Raveendran, J. Chen, Wearable triboelectric nanogenerators for biomechanical energy harvesting. *Nano Energy* 77 (2020) 105303.

[8] J. Bian, N. Wang, J. Ma, Y. Jie, J. Zou, X. Cao, Stretchable 3D polymer for simultaneously mechanical energy harvesting and biomimetic force sensing. *Nano Energy* 47 (2018) 442-450.

[9] L. Xu, Y. Pang, C. Zhang, T. Jiang, X. Chen, J. Luo, W. Tang, X. Cao, Z.L. Wang, Integrated triboelectric nanogenerator array based on air-driven membrane structures for water wave energy harvesting. *Nano Energy* 31 (2017) 351-358.

[10] S. Niu, X. Wang, F. Yi, Y.S. Zhou, Z.L. Wang, A universal self-charging system driven by random biomechanical energy for sustainable operation of mobile electronics. *Nat. Commun.* 6 (2015) 8975.

[11] J. Zhao, H. Guo, Y.K. Pang, F. Xi, Z.W. Yang, G. Liu, T. Guo, G. Dong, C. Zhang, Z.L. Wang, Flexible Organic Tribotronic Transistor for Pressure and Magnetic Sensing. *Acs Nano* 11 (2017) 11566-11573.

[12] S. Wang, Y. Xie, S. Niu, L. Lin, Z.L. Wang, Freestanding Triboelectric-Layer-Based Nanogenerators for Harvesting Energy from a Moving Object or Human Motion in Contact and Non-contact Modes. *Adv. Mater.* 26 (2014) 2818-2824.

[13] Y. Yang, Y.S. Zhou, H. Zhang, Y. Liu, S. Lee, Z.L. Wang, A Single-Electrode Based Triboelectric Nanogenerator as Self-Powered Tracking System. *Adv. Mater.* 25 (2013) 6594-6601.

[14] B. Meng, W. Tang, Z.-h. Too, X. Zhang, M. Han, W. Liu, H. Zhang, A transparent single-friction-surface triboelectric generator and self-powered touch sensor. *Energy Environ. Sci* 6 (2013) 3235-3240.

[15] S. Wang, L. Lin, Y. Xie, Q. Jing, S. Niu, Z.L. Wang, Sliding-Triboelectric Nanogenerators Based on In-Plane Charge-Separation Mechanism. *Nano Lett.* 13 (2013) 2226-2233.

[16] H. Guo, M.-H. Yeh, Y. Zi, Z. Wen, J. Chen, G. Lin, C. Hu, Z.L. Wang, Ultralight Cut-Paper-Based Self-Charging Power Unit for Self-Powered Portable Electronic and Medical Systems. *Acs Nano* 11 (2017) 4475-4482.

[17] H. Guo, Z. Wen, Y. Zi, M.-H. Yeh, J. Wang, L. Zhu, C. Hu, Z.L. Wang, A Water-Proof Triboelectric-Electromagnetic Hybrid Generator for Energy Harvesting in Harsh Environments. *Adv. Energy Mater* 6 (2016) 1501593.

[18] Y. Xie, S. Wang, S. Niu, L. Lin, Q. Jing, J. Yang, Z. Wu, Z.L. Wang, Grating-Structured Freestanding Triboelectric-Layer Nanogenerator for Harvesting Mechanical Energy at 85% Total Conversion Efficiency. *Adv. Mater.* 26 (2014) 6599-6607.

[19] Y. Xi, J. Wang, Y. Zi, X. Li, C. Han, X. Cao, C. Hu, Z. Wang, High efficient harvesting of underwater ultrasonic wave energy by triboelectric nanogenerator. *Nano Energy* 38 (2017) 101-108.

[20] L.-B. Huang, W. Xu, J. Hao, Energy Device Applications of Synthesized 1D Polymer Nanomaterials. *Small* 13 (2017) 1701820.

[21] W. Tang, Y. Han, C.B. Han, C.Z. Gao, X. Cao, Z.L. Wang, Self-Powered Water Splitting Using Flowing Kinetic Energy. *Adv. Mater.* 27 (2015) 272-276.

[22] W. Xu, M.-C. Wong, J. Hao, Strategies and progress on improving robustness and reliability of triboelectric nanogenerators. *Nano Energy* 55 (2019) 203-215.

[23] X.-S. Zhang, M.-D. Han, B. Meng, H.-X. Zhang, High performance triboelectric nanogenerators based on large-scale mass-fabrication technologies. *Nano Energy* 11 (2015) 304-322.

[24] M. Kanik, M.G. Say, B. Daglar, A.F. Yavuz, M.H. Dolas, M.M. El-Ashry, M. Bayindir, A Motion- and Sound-Activated, 3D-Printed, Chalcogenide-Based Triboelectric Nanogenerator. *Adv. Mater.* 27 (2015) 2367-2376.

[25] J. Wang, B. Wu, G. Liu, T. Bu, T. Guo, Y. Pang, X. Fu, J. Zhao, F. Xi, C. Zhang, Flexure hinges based triboelectric nanogenerator by 3D printing. *Extreme Mech. Lett.* 20 (2018) 38-45.

[26] H. Li, R. Li, X. Fang, H. Jiang, X. Ding, B. Tang, G. Zhou, R. Zhou, Y. Tang, 3D printed flexible triboelectric nanogenerator with viscoelastic inks for mechanical energy harvesting. *Nano Energy* 58 (2019) 447-454.

[27] H. Qiao, Y. Zhang, Z. Huang, Y. Wang, D. Li, H. Zhou, 3D printing individualized triboelectric nanogenerator with macro-pattern. *Nano Energy* 50 (2018) 126-132.

[28] Y. Su, J. Wang, B. Wang, T. Yang, B. Yang, G. Xie, Y. Zhou, S. Zhang, H. Tai, Z. Cai, G. Chen, Y. Jiang, L.-Q. Chen, J. Chen, Alveolus-Inspired Active Membrane Sensors for Self-Powered Wearable Chemical Sensing and Breath Analysis. *Acs Nano* 14 (2020) 6067-6075.

[29] Y. Su, T. Yang, X. Zhao, Z. Cai, G. Chen, M. Yao, K. Chen, M. Bick, J. Wang, S. Li, G. Xie, H. Tai, X. Du, Y. Jiang, J. Chen, A wireless energy transmission enabled wearable active acetone biosensor for non-invasive prediabetes diagnosis. *Nano Energy* 74 (2020) 104941.

[30] B. Chen, W. Tang, T. Jiang, L. Zhu, X. Chen, C. He, L. Xu, H. Guo, P. Lin, D. Li, J. Shao, Z.L. Wang, Three-dimensional ultraflexible triboelectric nanogenerator made by 3D printing. *Nano Energy* 45 (2018) 380-389.

[31] J.P. Lee, B.U. Ye, K.N. Kim, J.W. Lee, W.J. Choi, J.M. Baik, 3D printed noise-cancelling triboelectric nanogenerator. *Nano Energy* 38 (2017) 377-384.

[32] C. Qian, L. Li, M. Gao, H. Yang, Z. Cai, B. Chen, Z. Xiang, Z. Zhang, Y. Song, All-printed 3D hierarchically structured cellulose aerogel based triboelectric nanogenerator for multi-functional sensors. *Nano Energy* 63 (2019) 103885.

[33] J.H. Lee, R. Hinchet, S.K. Kim, S. Kim, S.-W. Kim, Shape memory polymer-based self-healing triboelectric nanogenerator. *Energy Environ. Sci* 8 (2015) 3605-3613.

[34] R. Liu, X. Kuang, J. Deng, Y.-C. Wang, A.C. Wang, W. Ding, Y.-C. Lai, J. Chen, P. Wang, Z. Lin, H.J. Qi, B. Sun, Z.L. Wang, Shape Memory Polymers for Body Motion Energy Harvesting and Self-Powered Mechanosensing. *Adv. Mater.* 30 (2018) 1705195.

[35] X. Dai, L.-B. Huang, Y. Du, J. Han, Q. Zheng, J. Kong, J. Hao, Self-Healing, Flexible, and Tailorable Triboelectric Nanogenerators for Self-Powered Sensors based on Thermal Effect of Infrared Radiation. *Adv. Funct. Mater.* 30 (2020) 1910723.

[36] W. Xu, M.-C. Wong, Q. Guo, T. Jia, J. Hao, Healable and shape-memory dual functional polymers for reliable and multipurpose mechanical energy harvesting devices. *J. Mater. Chem. A* 7 (2019) 16267-16276.

[37] W. Xu, L.-B. Huang, J. Hao, Fully self-healing and shape-tailorable triboelectric nanogenerators based on healable polymer and magnetic-assisted electrode. *Nano Energy* 40 (2017) 399-407.

[38] W. Xu, L.-B. Huang, M.-C. Wong, L. Chen, G. Bai, J. Hao, Environmentally Friendly Hydrogel-Based Triboelectric Nanogenerators for Versatile Energy Harvesting and Self-Powered Sensors. *Adv. Energy Mater* 7 (2017) 1601529.

[39] Z. Chen, D. Zhao, B. Liu, G. Nian, X. Li, J. Yin, S. Qu, W. Yang, 3D Printing of Multifunctional Hydrogels. *Adv. Funct. Mater.* 29 (2019) 1900971.

[40] S.-C. Zhao, M. Maas, K. Jansen, M. van Hecke, 3D Printed Actuators: Reversibility, Relaxation, and Ratcheting. *Adv. Funct. Mater.* 29 (2019) 1905545.

[41] L. Huang, R. Jiang, J. Wu, J. Song, H. Bai, B. Li, Q. Zhao, T. Xie, Ultrafast Digital Printing toward 4D Shape Changing Materials. *Adv. Mater.* 29 (2017) 1605390.

[42] A. Kirillova, R. Maxson, G. Stoychev, C.T. Gomillion, L. Ionov, 4D Biofabrication Using Shape-Morphing Hydrogels. *Adv. Mater.* 29 (2017) 1703443.

[43] D.L. Taylor, M.I.H. Panhuis, Self-Healing Hydrogels. *Adv. Mater.* 28 (2016) 9060-9093.

[44] A.S. Gladman, E.A. Matsumoto, R.G. Nuzzo, L. Mahadevan, J.A. Lewis, Biomimetic 4D printing. *Nat. Mater.* 15 (2016) 413-418.

[45] M. Champeau, D.A. Heinze, T.N. Viana, E.R. de Souza, A.C. Chinellato, S. Titotto, 4D Printing of Hydrogels: A Review. *Adv. Funct. Mater.* 30 (2020) 1910606.

[46] X. Kuang, D.J. Roach, J. Wu, C.M. Hamel, Z. Ding, T. Wang, M.L. Dunn, H.J. Qi, Advances in 4D Printing: Materials and Applications. *Adv. Funct. Mater.* 29 (2019) 1805290.

[47] X. Wan, L. Luo, Y. Liu, J. Leng, Direct Ink Writing Based 4D Printing of Materials and Their Applications. *Adv. Sci.* 7 (2020) 2001000.

[48] Y. Kim, H. Yuk, R. Zhao, S.A. Chester, X. Zhao, Printing ferromagnetic domains for untethered fast-transforming soft materials. *Nature* 558 (2018) 274-279.

[49] X. Kuang, K. Chen, C.K. Dunn, J. Wu, V.C.F. Li, H.J. Qi, 3D Printing of Highly Stretchable, Shape-Memory, and Self-Healing Elastomer toward Novel 4D Printing. *ACS Appl. Mater. Interfaces* 10 (2018) 7381-7388.

[50] L.-B. Huang, G. Bai, M.-C. Wong, Z. Yang, W. Xu, J. Hao, Magnetic-Assisted Noncontact Triboelectric Nanogenerator Converting Mechanical Energy into Electricity and Light Emissions. *Adv. Mater.* 28 (2016) 2744-2751.

[51] L.-b. Huang, W. Xu, G. Bai, M.-C. Wong, Z. Yang, J. Hao, Wind energy and blue energy harvesting based on magnetic-assisted noncontact triboelectric nanogenerator. *Nano Energy* 30 (2016) 36-42.

[52] C. Yan, Y. Gao, S. Zhao, S. Zhang, Y. Zhou, W. Deng, Z. Li, G. Jiang, L. Jin, G. Tian, T. Yang, X. Chu, D. Xiong, Z. Wang, Y. Li, W. Yang, J. Chen, A linear-to-rotary hybrid nanogenerator for high-performance wearable biomechanical energy harvesting. *Nano Energy* 67 (2020) 104235.

[53] C. Zhang, J. Chen, W. Xuan, S. Huang, B. You, W. Li, L. Sun, H. Jin, X. Wang, S. Dong, J. Luo, A.J. Flewitt, Z.L. Wang, Conjunction of triboelectric nanogenerator with induction coils as wireless power sources and self-powered wireless sensors. *Nat. Commun.* 11 (2020) 58.

[54] Z. Wang, J. An, J. Nie, J. Luo, J. Shao, T. Jiang, B. Chen, W. Tang, Z.L. Wang, A Self-Powered Angle Sensor at Nanoradian-Resolution for Robotic Arms and Personalized Medicare. *Adv. Mater.* 32 (2020) 2001466.

[55] X. Pu, H. Guo, Q. Tang, J. Chen, L. Feng, G. Liu, X. Wang, Y. Xi, C. Hu, Z.L. Wang, Rotation sensing and gesture control of a robot joint via triboelectric quantization sensor. *Nano Energy* 54 (2018) 453-460.

[56] S. Liu, Y. Li, W. Guo, X. Huang, L. Xu, Y.-C. Lai, C. Zhang, H. Wu, Triboelectric nanogenerators enabled sensing and actuation for robotics. *Nano Energy* 65 (2019) 104005.

Graphical abstracts

To further develop the wide utilization of Triboelectric Nanogenerators (TENGs), we introduce 4D printing technology and fabricate the transparent self-recovered TENGs, which not only provide excellent self-recoverability of device performance and improve the robustness of device structure, but also open a path to fabricate complicated structure through computer design with no need of any molds. The self-recovered TENGs based on 4D printing technology may offer great potential in energy harvesting and self-powered sensors for human-robot cooperation in sensing and control of robot in need of sophisticated and precise structures.